2024 IEEE International Conference on Robotics and Automation (ICRA 2024)
May 13-17, 2024. Yokohama, Japan

Optimized Design and Fabrication of Skeletal Muscle Actuators for Bio-syncretic Robots

Lianchao Yang, Chuang Zhang, *Member, IEEE*, Ruiqian Wang, Yiwei Zhang, and Lianqing Liu, *Member, IEEE*

Abstract— **In recent years, bio-syncretic robots actuated by living materials have received widespread attention. Among the common living materials, engineered skeletal muscle tissue (eSKT) has been the focus of researchers due to its high contraction force and good controllability. However, the current performance of eSKT is far from that of natural skeletal muscle tissue. In this paper, an optimized design method for eSKTs has been proposed. By combining simulation analysis with experiments, the eSKTs with multiple strips have been developed. The results show that under a specific volume (250 μL), the optimized strip structures can enhance the stability of eSKT and facilitate the penetration of nutrients and oxygen, leading to improved fusion of myoblasts and the directional arrangement of myotubes, thus improving the performance of eSKT. The eSKT with multiple strips exhibits a significant contraction force and has been successfully utilized in a bio-syncretic robot to demonstrate its actuation capability. This work may provide insights into the development of the field of bio-syncretic robots and even tissue engineering.**

I. Introduction

Since the emergence of robots in the mid-20th century, with the vigorous development of science and technology, the field of robots has been constantly innovating, and new robot paradigms have emerged [1]. Today, robots have been integrated into all aspects of people's lives, and play an important role in industry, medicine, services, and the military [2]. However, the development of traditional robots still faces many challenges. For example, traditional robots actuated by motors have low energy efficiency [3]. Generally, rigid robots lack flexibility and intrinsic safety when interacting with human. Traditional robots have difficulty maintaining effective driving force or time at the microscale. Nature always brings inspiration. Nature has endowed organisms with various advantages over traditional robots based on electromechanical systems. For example, organisms can efficiently convert chemical energy into mechanical energy output. Under the control of the nervous system, organisms can perform flexible complex movements. Organisms have good size scalability, allowing for actuation, perception and intelligence at the micro- and nanoscale [4]. With the advancement of technologies such as biofabrication and soft material synthesis, researchers are attempting to apply living materials to robotic research to overcome the challenges facing robotics development today.

Recently, a new type of robot composed of living and nonliving materials, the bio-syncretic robot (bio-hybrid robot), has been proposed and received extensive attention from the scientific community [5]. For example, Xi et al. integrated cardiomyocytes with a miniature silicon skeleton and pioneered the construction of a bio-syncretic robot that can move spontaneously. Actuated by cardiomyocytes, the robot's movement speed can reach 38 μm/s [6]. Subsequently, researchers applied eSKT [7-11], insect dorsal vascular tissue [12, 13], microorganisms [14-18] and blood cells [19-21] to bio-syncretic robotics research and constructed many impressive bio-syncretic robots. Among them, eSKT has been widely used due to its high driving force and good controllability. For example, Cvetkovic et al. combined eSKT with an asymmetric hydrogel skeleton to construct a bio-syncretic robot that can perform unidirectional motion. Under electrical stimulation, the eSKT can drive the robot to walk at a maximum speed of 156 μm/s [7]. Inspired by the organisms, Morimoto et al. constructed a bio-syncretic robot actuated by a pair of antagonistic eSKTs. The robot can perform operations such as picking and releasing objects [22]. Guix et al. integrated eSKT with a PDMS serpentine spring skeleton and constructed a bio-syncretic robot with high motion speed. The inherent energy storage properties of the spring shorten the contraction recovery time of the eSKT, allowing the eSKT to actuate the robot at high frequency. The robot can move at a maximum speed of 800 μm/s with 5 Hz electrical stimulation [23].

Although many eSKT-based bio-syncretic robots have been proposed, there are still some challenges that constrain their development. Currently, as the actuating core of bio-syncretic robots, the performance of eSKT is much smaller than that of natural skeletal muscle tissue, which hinders the improvement of bio-syncretic robot performance. To address this problem, researchers have proposed many optimized design methods. For example, Bian et al. constructed a PDMS mold with a series of pillars that can culture eSKT with large size, good repeatability and controllability. The pillars can make eSKT porous, thereby

Research supported by the National Key R&D Program of China (2022YFB4700100), National Natural Science Foundation of China (Grant Nos. 61925307, 62333021, and 62003338), National Defense Science and Technology Innovation Key deployment project of Chinese Academy of Sciences (Grant No. JCPYJJ-22020), CAS Project for Young Scientists in Basic Research (Grant No. YSBR-041), Youth Innovation Promotion Association, Chinese Academy of Science (Grant No. 2023210), State Key Laboratory of Robotics (2024-Z04) and Key Laboratory of Precision Diagnosis and Treatment of Gastrointestinal Tumors, Ministry of Education, China Medical University (GIPD-22-01).

L. Yang, R. Wang and Y. Zhang are with the State Key Laboratory of Robotics, Shenyang Institute of Automation, Chinese Academy of Sciences, Shenyang, 110016, Institutes for Robotics and Intelligent Manufacturing, Chinese Academy of Sciences, Shenyang, 110016, China and University of Chinese Academy of Sciences, Beijing 100049, China. (e-mail: yanglianchao@sia.cn, wangruiqian@sia.cn and zhangyiwei@sia.cn).

C. Zhang and L. Liu are with the State Key Laboratory of Robotics, Shenyang Institute of Automation, Chinese Academy of Science, Shenyang, 10016, China. (email: zhangchuang@sia.cn, lqliu@sia.cn).

* C. Zhang and L. Liu are the corresponding authors.

efficiently promoting the diffusion of nutrients and oxygen and improving the activity of the cells. The proposed mold was able to culture eSKTs with a large thickness, large area and high contraction force [24]. Morimoto et al. developed a method for constructing eSKTs with a high cross-sectional area and a multistrip structure. First, hydrogel sheets with myoblasts were prepared by a PDMS mold. Then, multiple hydrogel sheets were stacked on the structure with anchors. This method ensured gaps between the different muscle strips, thus promoting the diffusion of nutrients and oxygen. The results showed that eSKT cultured with this method had higher performance than eSKT without strip structure. Its tetanic force can exceed 10 mN [22]. In addition, Ren et al. proposed a method by which a multidegree-of-freedom eSKT bioactuator can be constructed. In this study, a device that can be expanded and curled was constructed. The device expanded when the eSKTs were cultured and curled when the eSKTs were mature, resulting in a bioactuator containing eight eSKTs [25].

ESKTs with large volumes and high contraction forces can be effectively constructed by the above methods. However, the fabrication process of these methods tends to be complicated. In addition, the structure of eSKT is highly customized, so it is difficult to integrate flexibly with nonliving materials. In this work, an eSKT optimization design method was proposed. First, four specific culture molds were constructed, using which modular eSKT with multiple strips can be manufactured. Then, by innovatively combining finite element simulation analysis with experimentation, the stability of eSKTs was analyzed, which is expected to improve the design efficiency of eSKTs and reduce experimental costs. Subsequently, the fabricated eSKTs were characterized by fluorescence staining and contraction force measurements. The results showed that under a specific volume (approximately 250 μL), eSKTs with multiple strips have better stability, differentiation effects and higher contraction forces than eSKTs without striped structures. Finally, the fabricated eSKT was integrated with a polydimethylsiloxane (PDMS) structure to construct a bio-syncretic robot capable of unidirectional movement. Under electrical stimulation, the eSKT contracts, thereby driving the robot to move at a speed of 698.09 μm/s. This work can bring unique insights to fields such as bio-syncretic robots and even tissue engineering.

The rest of the paper is organized as follows. Section II introduces the optimization strategy presented in this study; Section III provides the material and method; Section IV analyzes the experimental results; In Section V this study is discussed. The conclusion is finally presented in Section VI.

II. Optimization Strategy

The shapes of commonly used eSKTs in the research of bio-syncretic robots are mainly ring-shaped and strip-shaped. In the ring-shaped eSKT, myotubes distribute circularly, leading to contraction towards the center after electrical stimulation. However, while the contraction force is effective, the contraction displacement is small. The strip-shaped eSKT is characterized by a myotube distribution that resembles that of human spindle muscles, such as the biceps (Fig. 1), consisting of myotubes organized in series along the long axis and multiple parallel myotubes within the same cross-section. This unique structure enables contraction along the long axis when subjected to electrical stimulation, leading to larger contraction displacements and forces. The magnitude of the contraction force in strip-shaped eSKT is directly linked to the number of myotubes present in the cross-section. Therefore, theoretically, as long as the cross-sectional area of eSKT is increased, its contraction force can be increased. However, in contrast to human skeletal muscle, eSKT lacks a vascular network, resulting in limitations in nutrient and oxygen penetration depth. This constraint hampers the lateral growth of eSKT and subsequently impacts the output of contraction force.

Although some studies have successfully constructed relatively large eSKTs with good contractility through exquisite design [22, 24], these structures are highly customized and not easily applicable to the research of bio-syncretic robots. To address these limitations, a modular eSKT with multiple strips was proposed, which not only offered a large contraction displacement but also possessed a larger cross-sectional area while ensuring the diffusion of oxygen and nutrients, resulting in a higher contraction force. Moreover, the modular eSKT can be easily assembled with nonliving materials, facilitating the flexible construction of bio-syncretic robots. The eSKT was fabricated using the mold forming method (Fig. 3), in which the pillars at both ends function as tendons to fix and prevent spontaneous shrinkage of the eSKT while also providing topographic guidance for cell alignment and myotube distribution along the long axis. The protruding structure in the middle of the mold was used to separate the wider eSKT and promote the penetration of oxygen and nutrients. The narrower strip structure helped align cells and ensured the distribution of myotubes along the long axis.

The fabrication and culture period of eSKT often takes up to half a month, so experiments aimed at optimizing the configuration of eSKT require a longer time and higher costs. To address this issue, this study proposed using finite element simulation software to analyze the stress distribution of eSKT before formal experiments, to accelerate the optimization process. After the eSKTs matured, fluorescence staining analysis and contractility characterization would be performed to verify the effectiveness of the optimized design.

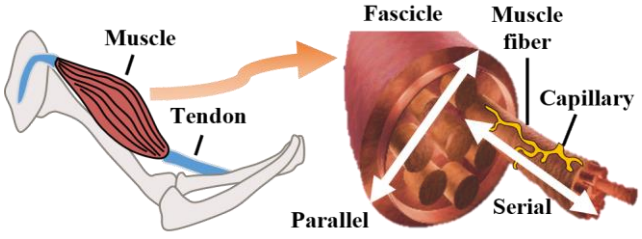

Figure 1. Schematic diagram of skeletal muscle and its microstructures.

III. Material and Method

A. Cell Preparation

Mouse myoblasts (C2C12) were purchased from American Type Culture Collection, Manassas, VA. C2C12 cells (less than five passages in age) were maintained in growth medium (GM) until they reached 80% confluency.

B. Fabrication of Culture Molds

First, the culture mold models were designed by computer-aided design software. According to the models, a polymethyl methacrylate (PMMA) negative mold was manufactured by a mini-type miller (Roland EGX-400; Japan). Then, the uncured PDMS (elastomer: curing agent = 10: 1) was poured into the PMMA negative mold and cured at 80 ℃ for 4 h. After PDMS polymerization, it was carefully separated from the PMMA negative mold to obtain the eSKT culture molds. Before the PDMS culture molds were used for eSKT culture, all molds needed to be sterilized by 75% ethanol solution, ultraviolet light irradiation, and soaked in phosphate buffered saline (PBS).

C. Fabrication and Culture of ESKT

Myoblasts were detached from culture dishes by 0.25% trypsin-EDTA (Gibco; America) when they reached approximately 80% confluency. Then, they were centrifuged, the supernatant was discarded, and the cells were washed into suspension with a small amount of GM. The suspension with a final cell density of 1×10^7 cells/mL was mixed with GM, Matrigel, fibrinogen and thrombin. Then, the suspension was poured into culture molds and transferred into an incubator. After one hour, the mixed material polymerized, and the GM was poured into culture dishes. After three days, the GM was changed to differentiation medium (DM). The DM was changed every two days to ensure that the myoblasts were well differentiated. On approximately the 6th or 7th day of differentiation, the spontaneous contraction of the eSKT was obvious, and it could be used to drive bio-syncretic robots.

D. Measurement of the Young's Modulus of ESKT by Atomic Force Microscope (AFM)

The Young's Modulus of eSKT was measured by a commercial AFM system called JPK NanoWizard (Bruker, Santa Barbara, CA, USA). The AFM probe used was MLCT-E (Bruker, Santa Barbara, CA, USA), which is made of silicon nitride, with an elastic coefficient of the probe's cantilever beam of 0.1 N/m. The measurement steps are as follows: 1) the AFM probe was pressed into the surface of the Petri dish in PBS to obtain force curves, thus the exact spring constant of the probe cantilever beam can be determined; 2) the Petri dish containing eSKT was transferred to the AFM sample stage and the suitable position for measurement was found with the help of an optical microscope; 3) the ramp velocity of the AFM probe was set to 2 μm/s, and the AFM probe was moved to indent the eSKT. More than 20 force curves were obtained on the eSKT to characterize its Young's modulus [26].

E. Immunofluorescence Staining

To analyze myoblast differentiation in different eSKTs, the myosin heavy chain (MyHC) protein was labeled with the reagents of Anti-Myosin Heavy Chain Alexa Fluor 488 (eBioscience). The specific steps are as follows [9]: 1) the eSKT was washed 3 times with PBS, each for 5 min; 2) the eSKT was fixed with immunostaining fixative (Beyotime) for 10 min; 3) the eSKT was then washed 3 times with immunostaining washing solution (Beyotime), each for 5 min; 4) the Anti-Myosin Heavy Chain Alexa Fluor 488 was diluted to 1% immunostaining solution with secondary antibody dilution buffer (Beyotime), and then the eSKT was covered with immunostaining solution for 1 h in dark environment; 5) the staining solution was removed, and the eSKT was washed three times with immunostaining washing solution, each for 5 min; and 6) the eSKT was covered with PBS and imaged using a commercial fluorescence microscope (Ti-e; Nikon, Tokyo, Japan).

F. Contraction Force Measurement of ESKTs by Force Sensor

On the 6th/7th day of differentiation, eSKTs exhibited obvious spontaneous contraction and regular contraction under electrical stimulation. To measure the contraction force of eSKTs, a system based on a high-precision force sensor (LSB200, FUTEK) was constructed (Fig. 2a), which consists of a force sensor, a data acquisition device, an electrical signal generator, a laptop, two carbon electrodes and some resin structures. When the eSKT matured, it was carefully peeled off and transferred into this system (Fig. 2b). Under electrical stimulation, eSKT contracts, and its isometric contraction force will be acquired and analyzed.

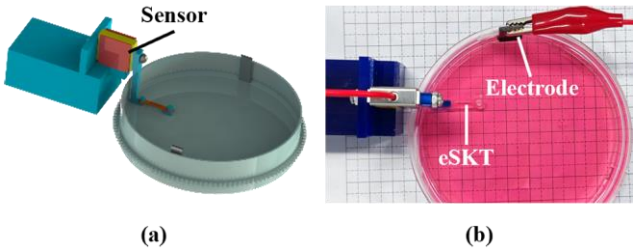

Figure 2. System for eSKT contraction force measurement. (a) Schematic diagram of force measuring system; (b) Physical diagram of force measuring system.

IV. Result

A. Design and Fabrication of ESKT

The casting method is commonly used to construct eSKTs. First, mixed biomaterials, including myoblasts, GM, Matrigel, fibrinogen and thrombin, are injected into a culture mold. Subsequently, the mixed biomaterials are polymerized and compacted under the traction of myoblasts. Finally, an eSKT with a specific configuration is obtained [7]. To construct eSKTs with different configurations, corresponding culture molds were designed by computer-aided design software (Fig. 3). These molds were fabricated through the PDMS casting method, and their volumes were approximately the same (248.82 μL, 249.00 μL, 251.05 μL and 249.29 μL, respectively) to minimize experimental variables. The molds

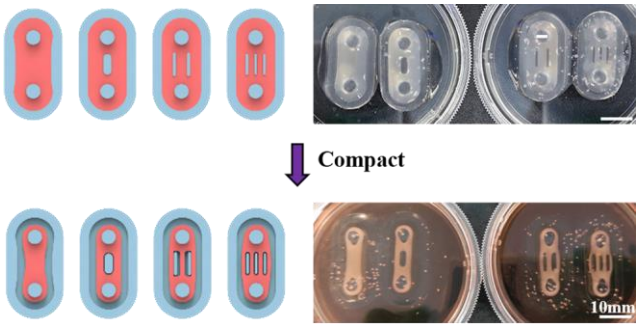

Figure 3. The eSKTs culture molds and culture process.

consisted of two 3.5 mm diameter pillars at the ends, which served to anchor the eSKT and prevent spontaneous shrinkage. Additionally, a protrusion in the middle of the molds was utilized to separate the eSKT into multiple strips. Compared to eSKTs with a single strip, the contact area with oxygen and nutrients was increased by 0.89, 4.85, and 8.53 mm^2 for eSKTs with double, triple, and quadruple strips, respectively, which might contribute to eSKT maturation.

B. *Stability Analysis of ESKT*

The stability of eSKTs in the study of eSKT-based bio-syncretic robots is a crucial consideration. Unstable configurations can lead to eSKT rupture, which hinders research progress. Therefore, the stability of eSKTs with different configurations was analyzed using finite element simulation and analysis software—COMSOL. The analysis procedure involved the following steps: 1) 3D models of eSKTs were constructed by computer-aided design software and then imported into COMSOL; 2) the material of the 3D models was designated as muscle, with Young's modulus set to the same value as that of eSKT, which was measured by AFM (Fig. 4a); 3) the Solid Mechanics Module was selected, and fixed constraints corresponding to eSKT in the culture mold were applied to specific boundaries of the 3D model, and 4) the traction force of myoblasts was substituted with body loads, and the stresses in each model were analyzed by a steady-state study. The results indicated that eSKTs with a single strip exhibited the highest stress, while those with multiple strips demonstrated lower stress levels (Fig. 4b). In fact, the single-strip eSKT was more prone to fracture during culture. Additionally, although the quadruple-strip eSKT displayed relatively low stress, its elongated strip structure made it susceptible to fracture as well (Fig. 4c). Similarly, this situation could also occur with the triple-strip eSKT. Consequently, the double-strip eSKT exhibited the highest stability, with a manufacturing success rate of 95% based on 20 experiments.

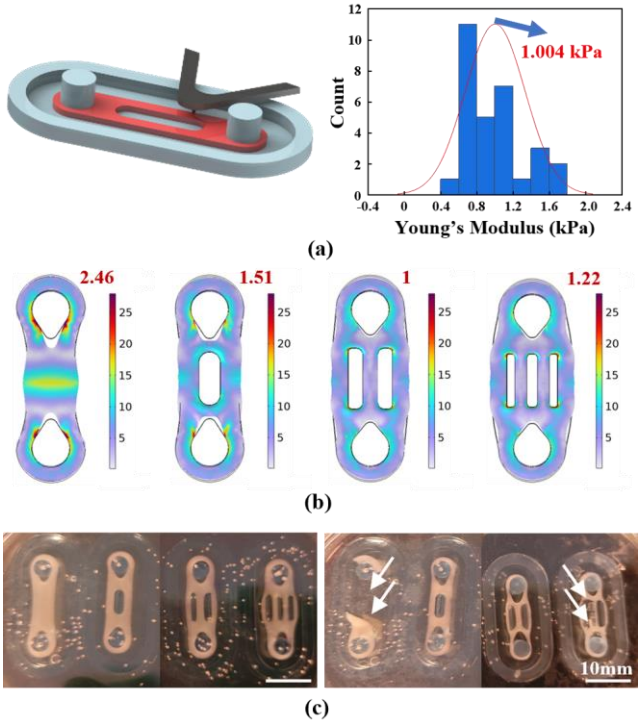

Figure 4. Analysis of eSKTs stability. (a) Schematic diagram of AFM measurement of Young's modulus of eSKT and Young's modulus curve; (b) Simulated stress distribution diagram of four types of eSKT; (c) Observation figures during the culture period, the left side is the first day after fabrication, and the right side is the fourth day after fabrication.

C. *Fluorescence Staining of ESKT*

On the 6th or 7th day of culture in DM, all eSKTs could contract under electrical stimulation. The MyHC of eSKT was stained with Anti-Myosin Heavy Chain Alexa Fluor 488 at this stage. Next, the eSKTs were imaged with a commercial laser scanning confocal microscope (Fig. 5a). The myotube alignment, width, and maturity of each eSKT were measured by ImageJ software and were statistically analyzed. In single-strip eSKT, the fusion of myoblasts was relatively random, resulting in few myotubes distributed in the direction of the extension axis (Fig. 5c). Closer to the center of the eSKT, the number of myotubes decreased, and the alignment decreased. This may be because internal myoblasts lack oxygen and nutrients [27, 28], thereby inhibiting the differentiation process. Additionally, internal myoblasts lack the traction constraints provided by anchoring pillars and cannot align well [29]. The eSKTs with double, triple and quadruple strips all exhibited a high degree of alignment (the angle between most of the myotubes and the extension axis was less than 5°), and there was no significant difference in the degree of alignment among them, indicating that the optimized molds can significantly improve the arrangement of myotubes. In single-strip eSKT, there was a significant difference in myotube width (Fig. 5d), which can be attributed to the random fusion of myoblasts. However, on the whole, the width of myotubes in single-strip eSKT was smaller. For double-, triple- and quadruple-strip eSKTs, there was no significant difference in myotube width among them.

Furthermore, the proportion of myotubes containing cross-striations (myofilaments and myofibrils in a specific order, as shown in Fig. 5b) was lowest in single-strip eSKT, which may indicate a lower degree of maturity (Fig. 5e) [30]. For double-, triple- and quadruple-strip eSKTs, this proportion was greater than that of single-strip eSKT. Among them, the double-strip eSKT exhibited the highest proportion. It should be noted that during the early stage of differentiation, myoblasts in narrow striped eSKT may have a higher contact probability [31], faster fusion rate, and earlier spontaneous contraction. This phenomenon is especially obvious in eSKT with triple or quadruple strips. However, during the mature stage, the double-strip eSKT not only ensures the fusion of myoblasts along the extension axis but also has more myoblasts in the horizontal direction. This may lead to better differentiation and higher maturity of double-strip eSKT. In addition, the double-strip eSKT was subjected to greater stress, which may provide appropriate mechanical stimulation to the eSKT, thereby promoting myoblast differentiation.

D. *Performance Characterization of ESKT*

A force measurement system based on a high-precision force sensor was designed to characterize the contraction force of eSKTs. The contraction force of the eSKT was measured at a frequency of 1 Hz under different electrical fields (Fig. 6a). The results showed that the contraction force of the

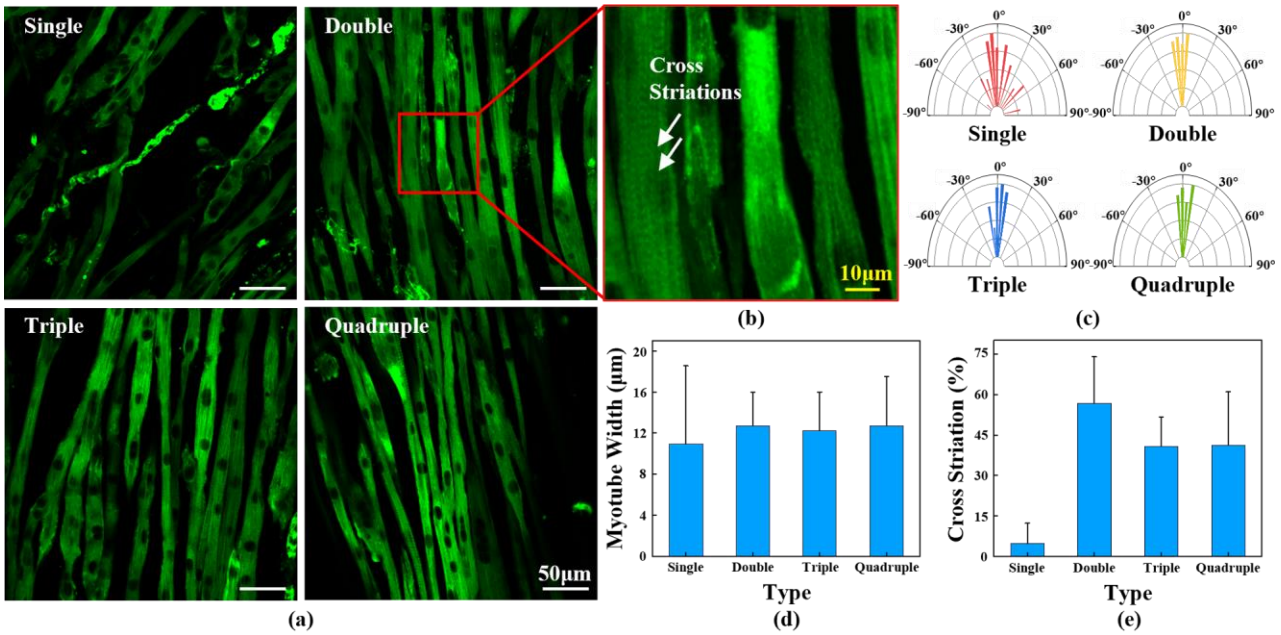

Figure 5. Characterization of eSKTs by fluorescence staining. (a) Fluorescence images of the four types of eSKT; (b) Fluorescence image with cross striations; (c) Comparison of myotube alignment between the four types of eSKT; (d) Comparison of myotube width between the four types of eSKT; (e) Comparison of the proportion of cross-striation structure among four types of eSKT.

eSKT first increases and then tends to be stable within a certain voltage range. This increase in force may be attributed to the activation of ion channels responsible for action potentials on the muscle cell membrane with increasing voltage. However, once the stimulation voltage reaches a certain threshold and the ion channels are fully open, the contraction force reaches its maximum and does not further increase [9]. It is important to note that excessively high voltages can lead to electrolysis of the culture medium and potential damage to the eSKT [32]; therefore, an excessive voltage is not desirable. Subsequently, the contraction force of eSKT at different lengths was measured at 3 V/cm, 1 Hz electrical field (Fig. 6b). As the length of the eSKT increased from 95% to 125% of its original length, its contraction force first increased and then decreased. At 110% of its original length, it had the maximum contraction force. This result has a guiding role in the construction of bio-syncretic robots.

Furthermore, under an appropriate electrical field of 3 V/cm, the contraction forces of four different types of eSKT were measured, counted and analyzed under different stimulation frequencies (Fig. 6c). The results indicated that the single-strip eSKT exhibited the lowest contraction force, while the multiple strip structure significantly enhanced the contraction force of the eSKTs. Among these structures, the double-strip eSKT demonstrated the highest contraction force. When subjected to electrical stimulation at a frequency of 25 Hz, its maximum tetanic force exceeded 500 μN. This result is consistent with the findings from the eSKT fluorescence staining experiment. In addition, these modular eSKTs can also be stacked and assembled to further improve the performance of bio-syncretic robots. The possibility of multiple modular eSKTs working together was further explored. As shown in Fig. 6d, two eSKTs arranged in parallel can produce greater contraction force than one eSKT, which provides ideas for constructing bio-syncretic robots with superior performance.

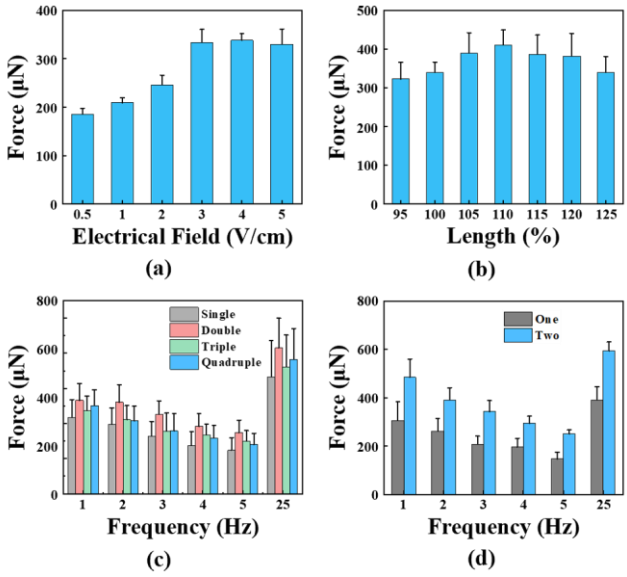

Figure 6. ESKTs performance characterization. (a) The relationship between the contraction force of the eSKT and electrical field; (b) The relationship between the contraction force of the eSKT and its length; (c) Comparison of the contraction force of the four types of eSKT under different stimulation frequencies; (d) Comparison of the contraction force between one eSKT and two eSKT under different stimulation frequencies.

E. Motion Demonstration of the Bio-syncretic Robot

The bio-syncretic robots were constructed using the double-strip eSKT due to its high stability and contraction force. A bio-syncretic robot composed of eSKT and PDMS structures, inspired by wriggling organisms such as caterpillars, was constructed (Fig. 7a). The PDMS structure consisted of two pillars of different sizes and thin films with grooves for connecting the pillars. The spacing between the two pillars was set to 110% of the original length of the eSKT to maximum its contraction force. The film was designed to

prevent the spontaneous shrinkage of the eSKT and maintain its effective contraction force. When electrically stimulated, the eSKT contracted, causing the film to bend, and the smaller pillar was lifted and titled down to the surface of the petri dish. At the same time, the friction force difference between the two pillars was generated, ultimately causing the robot to move in a single direction. By applying electrical pulse stimulation of 30 V and 3 Hz, the bio-syncretic robot achieved a maximum unidirectional speed of 698.09 μm/s (Fig. 7b).

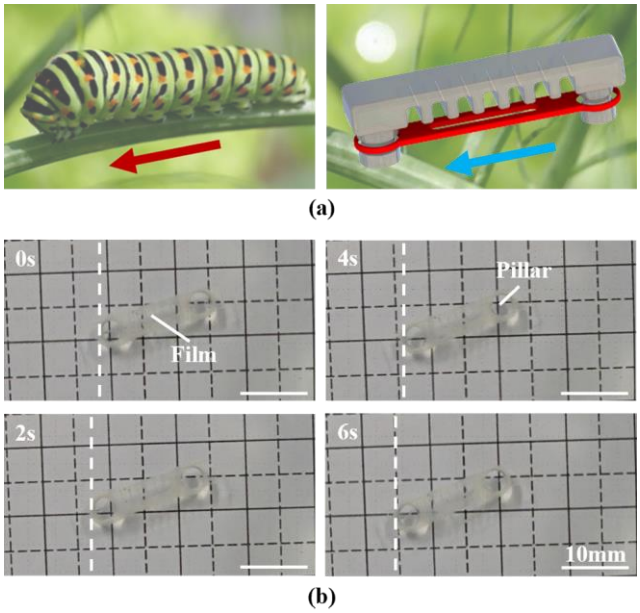

Figure 7. Bio-syncretic robot motion demonstration. (a) Schematic diagrams of the bio-syncretic robot; (b) Position change of the bio-syncretic robot between 0-6 s.

V. Discussion

An optimized design method of eSKT for bio-syncretic robot actuation was proposed in this study. The stress analysis of the eSKT was conducted using finite element simulation and analysis software. The experiments conducted on the fabricated eSKT with multiple strips confirmed its lower stress levels and higher culture stability. Furthermore, it was observed that the multiple strip structures facilitated the diffusion of oxygen and nutrients, improved the alignment of myotubes, and enhanced myoblast differentiation. However, it should be noted that the width of the strip in the double-strip eSKT showed favorable conditions for the fusion and differentiation of myoblasts only in a specific volume condition (approximately 250 μL before eSKT compaction), resulting in higher contraction efficiency. Increasing the volume of the eSKT may lead to better performance of an eSKT with a similar strip width and a greater number of strips compared to the double-strip eSKT. On the other hand, in the culture mode employed, the strip-shaped parts of the triple- and quadruple-strip eSKTs were affected by the protruding part, resulting in an arc-shaped formation that may not be conducive to the output of contraction force. Additionally, it was discovered that the stability of the eSKT depended on the widths of the circular parts at both ends and the striped parts in the middle, with the thinner part being more vulnerable to breakage. In this study, the double-strip eSKT was designed to achieve a balance between the two widths, resulting in its highest stability.

The main objective of this work is to fabricate an eSKT with an optimized structure and higher contraction force by combining simulation analysis and experimental verification, thereby laying a foundation for enhancing the performance of bio-syncretic robots. The introduction of finite element simulation analysis-assisted design can effectively accelerate the eSKT optimization process and reduce experimental costs. It is worth noting that this method is not only applicable to the eSKT shapes proposed in this study, but also useful in design of eSKT in other shapes.

The development of high-performance eSKT heavily relies on the ability to replicate the *in vivo* growth environment of natural muscle tissue. One crucial aspect for fabricating large and high-performance eSKT is the establishment of a vascular network that facilitates oxygen and nutrient supply, as well as waste transport. Although constructing eSKT with multiple strips can enhance the penetration of oxygen and nutrients, such a multi-strip structure provides only limited improvement compared to the dense vascular networks found in natural muscle tissue. Currently, vascularized muscle tissue has received widespread attention in the field of tissue engineering [33-35]. The introduction of vascular networks is expected to improve the existing culture conditions and fabricate large-sized, high performance eSKTs, thereby enhancing the performance of bio-syncretic robots.

VI. Conclusion

In this study, a modular eSKT with multiple strips that had been verified by simulation analysis and experiments was proposed. The use of a multi-strip structure effectively enhances the stability of the eSKT, facilitates the penetration of oxygen and nutrients, and promotes the alignment and differentiation of myoblasts into contractile myotubes. Compared to single-strip eSKT, the eSKT with multiple strips exhibits a greater contraction force, enabling it to drive a bio-syncretic robot to move at a fast speed (698.09 μm/s). Furthermore, this modular eSKT is easy to assemble with nonliving materials and can also be stacked to generate greater driving force, providing a solution for the flexible construction of high-performance bio-syncretic robots. This study not only has guiding significance for the research of bio-syncretic robots but can also provide insights into fields such as tissue engineering.

References

[1] L. Ricotti, B. Trimmer, A. W. Feinberg, R. Raman, K. K. Parker, R. Bashir, M. Sitti, S. Martel, P. Dario and A. Menciassi, "Biohybrid actuators for robotics: A review of devices actuated by living cells," *Sci Robot*, vol. 2, no. 12, p. eaaq0495, 2017.

[2] L. Yang, C. Zhang, R. Wang, Y. Zhang, W. Tan, and L. Liu, "Bio-Syncretic Robots Composed of Living-Electromechanical Systems," *Robot*, vol. 45, no. 1, pp. 89-109, 2023.

[3] V. Chan, H. H. Asada, and R. Bashir, "Utilization and control of bioactuators across multiple length scales," *Lab Chip*, vol. 14, no. 4, pp. 653-670, 2014.

[4] C. Zhang, W. Wang, N. Xi, Y. Wang, and L. Liu, "Development and future challenges of bio-syncretic robots," *Engineering*, vol. 4, no. 4, pp. 452-463, 2018.

[5] C. Zhang, J. Yang, W. Wang, and L. Liu, "Bio-syncretic robots composed of biological and electromechanical systems," *Nat. Sci. Rev.*, vol. 10, no. 5, Art. no. nwac274, 2023.

[6] J. Xi, J. J. Schmidt, and C. D. Montemagno, "Self-assembled microdevices driven by muscle," *Nat. Mater.*, vol. 4, no. 2, pp. 180-184, 2005.

[7] C. Cvetkovic, R. Raman, V. Chan, B. J. Williams, M. Tolish, P. Bajaj, M. S. Sakar, H. H. Asada, M. T. A. Saif and R. Bashir, "Three-dimensionally printed biological machines powered by skeletal muscle," *Proc. Natl. Acad. Sci. U. S. A*, vol. 111, no. 28, pp. 10125-10130, 2014.

[8] R. Raman, C. Cvetkovic, S. G. Uzel, R. J. Platt, P. Sengupta, R. D. Kamm and R. Bashir, "Optogenetic skeletal muscle-powered adaptive biological machines," *Proc. Natl. Acad. Sci. U. S. A*, vol. 113, no. 13, pp. 3497-3502, 2016.

[9] L. Liu, C. Zhang, W. Wang, N. Xi, and Y. Wang, "Regulation of C2C12 differentiation and control of the beating dynamics of contractile cells for a muscle-driven biosyncretic crawler by electrical stimulation," *Soft Robot*, vol. 5, no. 6, pp. 748-760, 2018.

[10] C. Zhang, Y. Zhang, W. Wang, N. Xi, and L. Liu, "A Manta Ray-Inspired Biosyncretic Robot with Stable Controllability by Dynamic Electric Stimulation," *Cyborg Bionic Syst*, vol. 2022, 2022.

[11] Y. Kim, Y. Yang, X. Zhang, Z. Li, A. Vázquez-Guardado, I. Park, J. Wang, A. I. Efimov, Z. Dou and Y. Wang, "Remote control of muscle-driven miniature robots with battery-free wireless optoelectronics," *Sci Robot*, vol. 8, no. 74, p. eadd1053, 2023.

[12] Y. Akiyama, K. Odaira, K. Sakiyama, T. Hoshino, K. Iwabuchi, and K. J. B. m. Morishima, "Rapidly-moving insect muscle-powered microrobot and its chemical acceleration," *Biomed. Microdevices.*, vol. 14, no. 6, pp. 979-986, 2012.

[13] Y. Yalikun, K. Uesugi, M. Hiroki, Y. Shen, Y. Tanaka, Y. Akiyama and K. Morishima, "Insect Muscular Tissue-Powered Swimming Robot," *Actuators*, vol. 8, no. 2, p. 30, 2019.

[14] D. B. Weibel, P. Garstecki, D. Ryan, W. R. Diluzio, M. Mayer, J. E. Seto and G. M. Whitesides,"Microoxen: Microorganisms to move microscale loads," *Proc. Natl. Acad. Sci. U. S. A,* vol. 102, no. 34, pp. 11963-11967, 2005.

[15] D. Akin J. Sturgis, K. Ragheb, D. Sherman, K. Burkholder, J. P. Robinson, A. K. Bhunia, S. Mohammed and R. Bashir, "Bacteria-mediated delivery of nanoparticles and cargo into cells," *Nat. Nanotechnol.*, vol. 2, no. 7, pp. 441-449, 2007.

[16] B. W. Park, J. Zhuang, O. Yasa, and M. Sitti, "Multifunctional Bacteria-Driven Microswimmers for Targeted Active Drug Delivery," Acs Nano, vol. 11, no. 9, pp. 8910-8923, 2017.

[17] Y. Alapan, O. Yasa, O. Schauer, J. Giltinan, A. F. Tabak, V. Sourjik and M. Sitti, "Soft erythrocyte-based bacterial microswimmers for cargo delivery," *Sci. Robot.*, vol. 3, no. 17, p. eaar4423, 2018.

[18] J. Li, L. Dekanovsky, B. Khezri, B. Wu, H. Zhou, and Z. Sofer, "Biohybrid Micro-and Nanorobots for Intelligent Drug Delivery," *Cyborg Bionic Syst*, vol. 2022, 2022.

[19] J. Han, J. Zhen, V. Du Nguyen, G. Go, Y. Choi, S. Y. Ko, J.-O. Park and S. Park, "Hybrid-actuating macrophage-based microrobots for active cancer therapy," *Sci. Rep.*, vol. 6, no. 1, pp. 1-10, 2016.

[20] H. Zhang, Z. Li, C. Gao, X. Fan, Y. Pang, T. Li, Z. Wu, H. Xie and Q. He, "Dual-responsive biohybrid neutrobots for active target delivery," *Sci. Robot.*, vol. 6, no. 52, p. eaaz9519, 2021.

[21] Z. G. Wu, T. L. Li, J. X. Li, W. Gao, T. L. Xu, C. Christianson, W. W. Gao, M. Galarnyk, Q. He, L. F. Zhang and J. Wang, "Turning Erythrocytes into Functional Micromotors," *Acs Nano*, vol. 8, no. 12, pp. 12041-12048, 2014.

[22] Y. Morimoto, H. Onoe, and S. Takeuchi, "Biohybrid robot powered by an antagonistic pair of skeletal muscle tissues," *Sci Robot*, vol. 3, no. 18, p. eaat4440, 2018.

[23] M. Guix, R. Mestre, T. Patiño, M. De Corato, J. Fuentes, G. Zarpellon and S. Sánchez, "Biohybrid soft robots with self-stimulating skeletons," *Sci Robot*, vol. 6, no. 53, p. eabe7577, 2021.

[24] W. Bian and N. Bursac, "Engineered skeletal muscle tissue networks with controllable architecture," *Biomaterials*, vol. 30, no. 7, pp. 1401-1412, 2009.

[25] X. Ren, Y. Morimoto, and S. Takeuchi, "3-DoF Biohybrid Actuator with Multiple Skeletal Muscle Tissues," in *2023 IEEE 36th International Conference on Micro Electro Mechanical Systems (MEMS)*. IEEE, 2023, pp. 201-204.

[26] Y. Feng and M. Li, "Micropipette-assisted atomic force microscopy for single-cell 3D manipulations and nanomechanical measurements," *Nanoscale*, 2023.

[27] E. C. Novosel, C. Kleinhans, and P. J. Kluger, "Vascularization is the key challenge in tissue engineering," *Adv. Drug. Deliver. Rev.*, vol. 63, no. 4-5, pp. 300-311, 2011.

[28] Y. Akiyama, A. Nakayama, S. Nakano, R. Amiya, and J. Hirose, "An electrical stimulation culture system for daily maintenance-free muscle tissue production," *Cyborg Bionic Syst*, vol. 2021, 2021.

[29] T. Nomura, M. Takeuchi, E. Kim, Q. Huang, Y. Hasegawa, and T. Fukuda, "Development of Cultured Muscles with Tendon Structures for Modular Bio-Actuators," *Micromachines*, vol. 12, no. 4, Apr 2021, Art. no. 379.

[30] A. Khodabukus, L.Madden, N. K. Prabhu, T. R. Koves, C. P. Jackman, D. M. Muoio and N. Bursac, "Electrical stimulation increases hypertrophy and metabolic flux in tissue-engineered human skeletal muscle," *Biomaterials*, vol. 198, pp. 259-269, 2019.

[31] Y. Sun, R. Duffy, A. Lee, and A. W. Feinberg, "Optimizing the structure and contractility of engineered skeletal muscle thin films," *Acta Biomater*, vol. 9, no. 8, pp. 7885-7894, 2013.

[32] M. Radisic, H.Park, T. P. Martens, J. E. Salazar-Lazaro, W. Geng, Y. Wang, R. Langer and L. E. Freed, "Pre - treatment of synthetic elastomeric scaffolds by cardiac fibroblasts improves engineered heart tissue," *J Biomed Mater Res A*, vol. 86, no. 3, pp. 713-724, 2008.

[33] H. Kim, T. Osaki, R. D. Kamm, and H. H. Asada, "Tri - culture of spatially organizing human skeletal muscle cells, endothelial cells, and fibroblasts enhances contractile force and vascular perfusion of skeletal muscle tissues," *FASEB J*, vol. 36, e22453, 2022.

[34] K. H. Nakayama et al., "Treatment of volumetric muscle loss in mice using nanofibrillar scaffolds enhances vascular organization and integration," *Commun. Biol.*, vol. 2, Art. no. 170, 2019.

[35] Q. Lian, T. Zhao, T. Jiao, Y. Huyan, H. Gu, and L. J. J. o. B. E. Gao, "Direct-writing process and in vivo evaluation of prevascularized composite constructs for muscle tissue engineering application," *J Bionic. Eng.*, vol. 17, no. 3, pp. 457-468, 2020.